DOI: 10.17516/1997-1397-2022-15-3-386-397
УДК 532

Perturbation Approach for a Flow over a Trapezoidal Obstacle

May Manal Bounif*
Abdelkader Gasmi†
Laboratory of Pure and Applied Mathematics
Faculty of Mathematics and Informatics
University of Msila
Msila, Algeria

Received 04.10.2021, received in revised form 10.11.2021, accepted 04.02.2022

Abstract. In this paper, we tackle the two-dimensional and irrotational flow of inviscid and incompressible fluid over a trapezoidal obstacle. The free surface of the flow which is governed by the Bernoulli condition is determined as a part of solution of the problem. This condition renders difficult an analytical solution of the problem. Hence, our work's objective is utilize the Hilbert transformation and the perturbation technique to provide an approximate solution to this problem for large Weber numbers and various configurations of the obstacle. The obtained results demonstrate that the used method is easily applicable, and provides approximate solutions to these kinds of problems.

Keywords: free surface flow, surface tension, incompressible flow, Hilbert method, perturbation technique.

Citation: M.M. Bounif, A. Gasmi, Perturbation Approach for a Flow over a Trapezoidal Obstacle, J. Sib. Fed. Univ. Math. Phys., 2022, 15(3), 386–397. DOI: 10.17516/1997-1397-2022-15-3-386-397.

Our study begins with a consideration of the steady two-dimensional and irrotational fluid flow over a trapezoidal obstacle. On the one hand, we assume the fluid is incompressible and inviscid. On the other hand, we consider the surface tension effect but neglect the effect of gravity. A major characteristic of the present problem is the nonlinear condition given through the Bernoulli equation on the free surface of an unknown shape. The latter can be identified as part of the solution to the problem. In addition, because this condition the proposed problem become difficult to solve it analytically, so it is necessary to look for an approximate solution to it.

Free-surface flow problems have been approached using different techniques and methods over the past few decades. Of these techniques and methods we can mention the series truncation technique and boundary integral method, which helps determine the free surface shape for potential flows over given obstacles. For example Forbes and Schwartz [1], determine the non-linear solutions of subcritical and supercritical flows over a semi-circular obstacle, Gasmi and Mekias [2], Gasmi and Amara [3] and Vanden-Broeck [4], studied the problems of flow over an obstruction in a channel, whilst Dias, Killer and Vanden-Broeck [5] , obtained solutions to both subcritical and supercritical free-surface flows past a triangular obstacle, Wiryanto [6] take the problem of the flow under a sluice gate, M.B. Abd-el-Malek and S. Z. Masoud [7] obtains

*maymanal.bounif@univ-msila.dz http://orcid.org/0000-0003-2530-6981
†abdelkader.gasmi@univ-msila.dz

the linear solution of the flow over a ramp, by representing the bottom in integral form using Fourier's double-integral theorem. M. B. Abd-el-Malek and S. N. Hanna [8] solved numerically the problem of the flow over a ramp with gravity effect by the Hilbert Method and the perturbation technique. M. B.Abd-el-Malek, S. N. Hanna and M. T. Kamel [9] investigated the flow over triangular bottom. Bounif and Gasmi [10] , on the other hand, examined the problem that involves a free-surface flows over a step at the bottom of a channel, they offered a solution to the problem using the perturbation method.

The method that we employ in this paper to approximate a solution of the considered problem follows three steps. Initially, we map the flow field of the physical plane onto the upper half plane using the Schwartz–Christoffel transformation. Accordingly, the Hilbert method helps us identify a system of nonlinear equation when applied to the new upper half plane's mixed-boundary value problem. Finally, the perturbation technique is utilized to provide a solution to the system for some large values of the Weber number and varied trapezoidal obstacle configurations. The employability of our method will then be clear given the acquired results, as it provides approximate solutions to the selected kind of problems.

The outline of the paper can be given in four main sections. The first of which will introduce the mathematical formulation of the present problem. Section 2 presents the approximation of equations of the problem, while Section 3 delineates the application of the perturbation technique to solve it. Finally, we show certain free streamline shapes and results in final section.

1. Formulation of problem

Let us consider the motion of a two-dimensional flow of a fluid over a trapezoidal obstacle. The fluid is assumed to be incompressible, irrotational and inviscid. The effect of gravity is neglected but we take into account the superficial tension effect. The flow we propose is uniform and has a constant discharge $U_1h_1 = U_2h_2$, where U_i, $i = 1, 2$ designates the velocities and h_i, $i = 1, 2$ are the depths of the flow upstream and downstream respectively. Hence, the bottom consists of the horizontal walls A_0A_{-1} and $A_1A^{'}$ and the asymmetric polygon $A_{-1}A_{-2}\dots A_{-N}A_N\dots A_2A_1$ of $2N$ angles α_i and $(2N-1)$ straight-line segments. Furthermore, we choose Cartesian coordinates with the origin in the point (see Fig. 1).

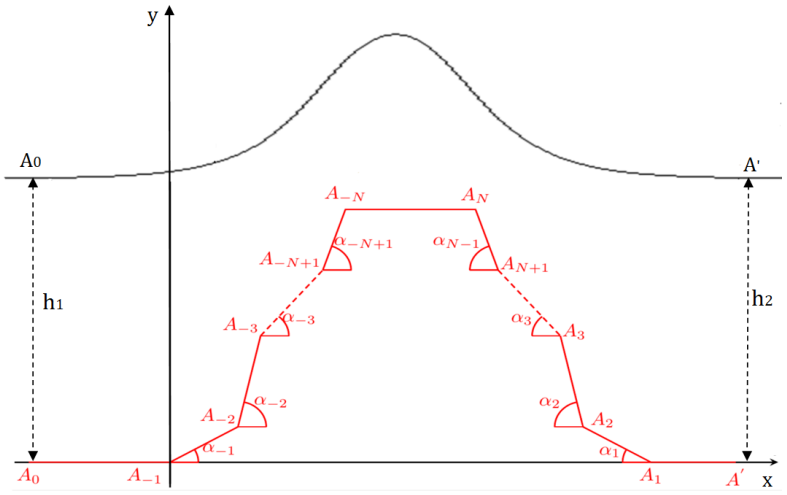

Fig. 1. Sketch of the flow and of the coordinates

The dimensionless variables are defined by choosing U_1 as the unit velocity and h_1 as the unit length. We introduce the complex potential $f(z) = \varphi(z) + i\psi(z)$, where φ is the potential function, ψ the stream function (φ and ψ are conjugate solutions of Laplace's equation) and $f(z)$ is an analytic function of z within the region of flow with complex conjugate velocity

$$\eta = \frac{df(z)}{dz} = u - iv = qe^{-i\theta}. \tag{1}$$

Let

$$\kappa = \ln \eta = \ln q - i\theta, \tag{2}$$

where κ is called the logarithmic hodograph variable. Then, from (1) and (2) we get

$$z = \int e^{-\omega} df. \tag{3}$$

Without loss of generality, we choose $\varphi = 0$ at a point A_{-1} , $\psi = 1$ on the streamline $A_0A^{'}$, and $\psi = 0$ on the streamline $A_0A_{-1}A_{-2}\ldots A_{-N}A_N\ldots A_1A^{'}$ (see Fig. 2). We denote the dimensionless trapezoid depth by r_i, where

$$r_i = l_i \sin(\alpha_i), \tag{4}$$

where

$$l_i = \begin{cases} |A_iA_{i-1}|, & i = -1, \ldots, -N+1, \\ |A_iA_{i+1}|, & i = 1, \ldots, N-1. \end{cases} \tag{5}$$

On the free-surface, where the pressure is uniform, the dimensionless form of the Bernoulli equation is given by:

$$q^2 + \frac{2}{We}\left|\frac{\partial\theta}{\partial\varphi}\right| q = 1, \tag{6}$$

where We is the adimensional parameter, known as the Weber number and defined by:

$$We = \frac{\rho U_1^2 h_1}{T}, \tag{7}$$

T is the surface tension, and ρ is the density of the fluid.

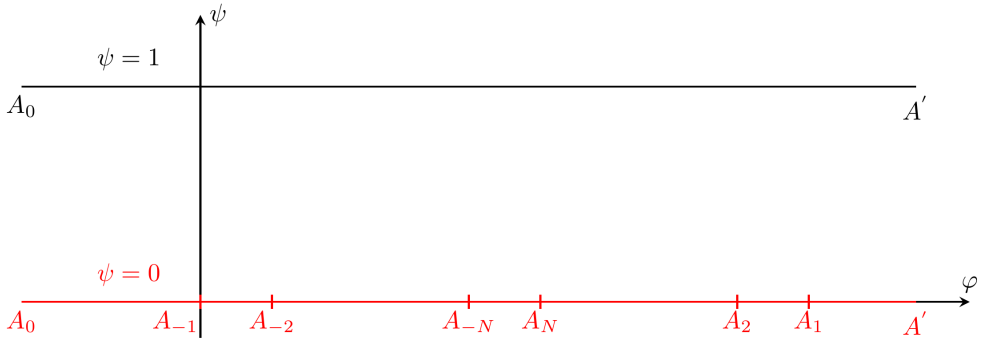

Fig. 2. The potential f plane

Using the Schwartz-Christoffel transformation, we map the potential plane f as seen in Fig. 2 onto the upper half of an auxiliary t-plane see Fig. 3.

The tranformation used is:

$$f(t) = -\frac{1}{\pi}\ln(1-t). \tag{8}$$

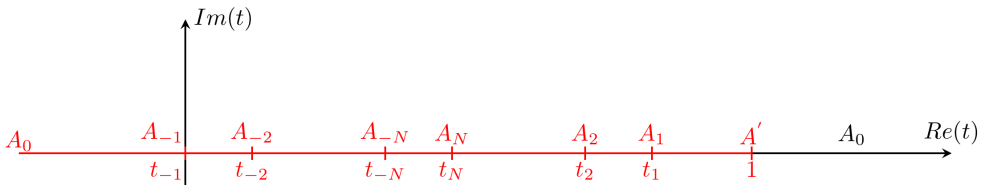

Fig. 3. The auxiliary t plane

1.1. The Hilbert method

In order to express κ as the single variable t function, we need to use the Hilbert method for the obtained mixed problem of the new plane. Hence, the solution for an analytic function $\chi(t)$ in the upper half-plane (see [11]) is given by

$$\chi(t) = \frac{1}{\pi} p.v. \int_{-\infty}^{+\infty} \frac{Im\left[\chi(s)\right]}{s-t} ds + \sum_{j=0}^{\infty} B_j t^j. \tag{9}$$

Where B_j are real constants and $p.v.$ is the principal value of the integral.
The real and imaginary parts of $\kappa(t)$ are given by

$$\begin{aligned} Im\left[\kappa(t)\right] &= -\theta(t), \\ Re\left[\kappa(t)\right] &= \ln q(t). \end{aligned} \tag{10}$$

Where

$$\theta(t) = \begin{cases} 0, & t < 0 = t_1, \\ \alpha_i, & t_i < t < t_{i-1}, \quad i = -N+1, \ldots, -1, \\ -\alpha_i, & t_{i+1} < t < t_i, \quad i = 1, \ldots, N-1, \\ 0, & t_N < t < 1, \\ \theta(t), & t > 1. \end{cases} \tag{11}$$

To switch the function $\kappa(t)$ to $\chi(t)$, we use an auxiliary function $H(t)$

$$H(t) = \begin{cases} \sqrt{1-t}, & t < 1, \\ -i\sqrt{t-1}, & t > 1. \end{cases} \tag{12}$$

Using (10) and (12), with $\chi(t) = \kappa(t)/H(t)$, we get

$$\chi(t) = \left\{ \begin{array}{ll} \dfrac{\ln q(t) - i\theta(t)}{\sqrt{1-t}}, & t < 1, \\ \dfrac{\ln q(t) - i\theta(t)}{-i\sqrt{t-1}}, & t > 1. \end{array} \right\} = U(t) + iV(t). \tag{13}$$

Examining the upstream condition, we have

$$B_j = 0, j = 0, 1, 2, \ldots .$$

and hence

$$\chi(t) = \frac{1}{\pi} p.v. \int_{-\infty}^{+\infty} \frac{Im\left[\chi(s)\right]}{s-t} ds. \tag{14}$$

Therefore, using (13) and (14), we obtain

$$U(t) = \frac{1}{\pi} p.v. \int_{-\infty}^{+\infty} \frac{V(s)}{s-t} ds. \tag{15}$$

$$V(t) = -\frac{1}{\pi} p.v. \int_{-\infty}^{+\infty} \frac{U(s)}{s-t} ds. \tag{16}$$

Along the real axis of the upper half-plane $Im(t) = 0$ (see Fig 3), the distribution of both real and imaginary parts of $\chi(t)$ can be recapitulated; check Tab. 1. Therefore, q_0 is defined in $t < 0$ and q_∞ is defined in $t_N < t < 1$.

Using (15), (16) and Tab. 1, we obtain the following systems of the nonlinear integral equations:

Table 1. Distribution of the flow quantities along $Im(t) = 0$

t	$U(t)$	$V(t)$
$t < 0 = t_{-1}$	$\frac{\ln q_0(t)}{\sqrt{1-t}}$	0
$t_i < t < t_{i-1}$; $i = -N+1, \ldots, -1$	$\frac{\ln q_i(t)}{\sqrt{1-t}}$	$\frac{-\alpha_i}{\sqrt{1-t}}$
$t_{i+1} < t < t_i$; $i = 1, \ldots, N-1$	$\frac{\ln q_i(t)}{\sqrt{1-t}}$	$\frac{\alpha_i}{\sqrt{1-t}}$
$t_N < t < 1$	$\frac{\ln q_\infty(t)}{\sqrt{1-t}}$	0
$t > 1$	$\frac{\theta(t)}{\sqrt{t-1}}$	$\frac{\ln q(t)}{\sqrt{t-1}}$

$$\begin{aligned} \theta(t) \quad &= \frac{\sqrt{t-1}}{\pi} p.v. \int_1^{+\infty} \frac{\ln q(s)}{(s-t)\sqrt{s-1}} ds + \sum_{i=-N+1}^{-1} \frac{2\alpha_i}{\pi} \tan^{-1}\left(\frac{(m_i - m_{i-1})\sqrt{t-1}}{t-1+m_i m_{i-1}}\right) - \\ &- \sum_{i=1}^{N-1} \frac{2\alpha_i}{\pi} \tan^{-1}\left(\frac{(m_{i+1} - m_i)\sqrt{t-1}}{t-1+m_{i+1} m_i}\right), \qquad t > 1, \end{aligned} \tag{17}$$

where

$$m_i = \sqrt{1-t_i}. \tag{18}$$

And

$$\begin{aligned} \ln(q_j(t)) \quad &= \quad \frac{\sqrt{1-t}}{\pi} \left\{ p.v. \int_1^{+\infty} \frac{\ln q(s)}{(s-t)\sqrt{s-1}} ds + \sum_{i=-N+1}^{-1} \alpha_i \int_{t_i}^{t_{i-1}} \frac{ds}{(s-t)\sqrt{1-s}} - \right. \\ &- \quad \left. \sum_{i=1}^{N-1} \alpha_i \int_{t_{i+1}}^{t_i} \frac{ds}{(s-t)\sqrt{1-s}} \right\}, \end{aligned} \tag{19}$$

where $p.v.$ is the principal value of the integral and for $j = -N, \ldots, -1$, $q_j(t)$ being the flow speed in $t_j < t < t_{j-1}$, and for $j = 1, \ldots, N$, $q_j(t)$ being the flow speed in $t_{j+1} < t < t_j$.

Using (3) and (8), the coordinates of a point on the free-surface can be obtained as follows:

$$z(t) = z_\infty - \frac{1}{\pi} \int_t^{+\infty} \frac{e^{i\theta(s)}}{(1-s)q(s)} ds, \quad t > 1. \tag{20}$$

By separating the real and imaginary parts, we get:

$$x(t) = x_\infty - \frac{1}{\pi}\int_t^{+\infty} \frac{\cos\theta(s)}{(1-s)q(s)}ds, \quad t>1, \tag{21}$$

$$y(t) = 1 - \frac{1}{\pi}\int_t^{+\infty} \frac{\sin\theta(s)}{(1-s)q(s)}ds, \quad t>1. \tag{22}$$

2. The approximate equations

In this section, we approximate the nonlinear integral equations (6), (17), (21) and (22) , when Weber number is large.

Using the first-order Taylor development with respect to $\frac{1}{We}\left|\frac{\partial\theta}{\partial\varphi}\right|$, we can give the solution to the Bernoulli equation as follows:

$$q(t) \approx 1 - \frac{1}{We}\left|\frac{\partial\theta}{\partial\varphi}\right|. \tag{23}$$

Using the relation (8), we obtain:

$$\frac{\partial\theta}{\partial\varphi} = \frac{\partial\theta}{\partial t}\frac{\partial t}{\partial\varphi} = \pi(t-1)\frac{\partial\theta}{\partial t}, \quad t>1. \tag{24}$$

Consequently, for $t>1$ the flow speed is approximated by

$$q(t) \approx 1 - \frac{\pi}{We}(t-1)\frac{\partial\theta}{\partial t}(t). \tag{25}$$

which yields

$$\ln q(t) \approx -\frac{\pi}{We}(t-1)\frac{\partial\theta}{\partial t}(t), \tag{26}$$

and

$$\frac{1}{q(t)} \approx 1 + \frac{\pi}{We}(t-1)\frac{\partial\theta}{\partial t}(t). \tag{27}$$

For small angles α_i, the change in θ will be minor, thus, allowing us to approximate $\sin\theta$ by $\theta(t)$ and $\cos\theta$ by one.

Using (26), we can approximate the angle of the free surface with the horizontal (17) by

$$\begin{aligned}\theta(t) \approx -\frac{\sqrt{t-1}}{We}p.v.\int_1^{+\infty}\frac{(s-1)\frac{\partial\theta}{\partial s}(s)}{(s-t)\sqrt{s-1}}ds + \sum_{i=-N+1}^{-1}\frac{2\alpha_i}{\pi}\tan^{-1}\left(\frac{(m_i-m_{i-1})\sqrt{t-1}}{t-1+m_im_{i-1}}\right) - \\ - \sum_{i=1}^{N-1}\frac{2\alpha_i}{\pi}\tan^{-1}\left(\frac{(m_{i+1}-m_i)\sqrt{t-1}}{t-1+m_{i+1}m_i}\right), \quad t>1,\end{aligned} \tag{28}$$

substituting (27) into (21) and (22), and after simplification, the free surface equations take the form:

$$\begin{aligned} x(t) &\approx x_\infty - \frac{1}{\pi}\int_t^{+\infty}\frac{1}{(1-s)}\left[1+\frac{\pi}{We}(s-1)\frac{\partial\theta}{\partial s}(s)\right]ds \\ &\approx x_\infty - \frac{1}{\pi}\int_t^{+\infty}\frac{1}{(1-s)}ds + \frac{1}{We}\left[\lim_{s\longrightarrow\infty}\theta(s) - \theta(t)\right] \\ &\approx x_\infty - \frac{1}{\pi}\int_t^{+\infty}\frac{1}{(1-s)}ds - \frac{1}{We}\theta(t), \end{aligned} \tag{29}$$

and

$$\begin{aligned} y(t) &\approx 1-\frac{1}{\pi}\int_t^{+\infty}\frac{\theta(s)}{(1-s)}\left[1+\frac{\pi}{We}(s-1)\frac{\partial\theta}{\partial s}(s)\right]ds \\ &\approx 1-\frac{1}{\pi}\int_t^{+\infty}\frac{\theta(s)}{(1-s)}ds+\frac{1}{2We}\left[\lim_{s\longrightarrow\infty}\theta^2(s)-\theta(t)^2\right] \\ &\approx 1-\frac{1}{\pi}\int_t^{+\infty}\frac{\theta(s)}{(1-s)}ds-\frac{\theta^2(t)}{2We}. \end{aligned} \tag{30}$$

To solve the system of the nonlinear integral equations (25), (28)–(30), we use the Perturbation technique.

3. Perturbation technique

We expand $X(t)$ in terms of the small parameters α_i

$$X(t)=\sum_{j=-N+1}^{N-1}\sum_{k=0}^{\infty}\alpha_j^k X_{k,\alpha_j}(t). \tag{31}$$

Where $X(t)$ stands for $q(t)$, $\theta(t)$, $\theta^{'}(t)$, $x(t)$ and $y(t)$.

3.1. Zero-order approximation

This case corresponds to the flow far upstream, which we consider as uniform. Then, the zero-order approximation of the nonlinear integral equations (25), (28)–(30) is presented by:

- The velocity of the flow
$$q_0(t)\approx 1-\frac{\pi}{We}(t-1)\theta_0^{'}(t)\approx 1. \tag{32}$$
- The velocity direction relative to the horizontal
$$\theta_0(t)\approx -\frac{\sqrt{t-1}}{We}p.v.\int_1^{+\infty}\frac{(s-1)\theta_0^{'}(s)}{(s-t)\sqrt{s-1}}ds\approx 0. \tag{33}$$
- The free streamline equations:
$$\begin{aligned} x_0(t) &\approx x_\infty-\frac{1}{\pi}\int_t^{+\infty}\frac{1}{(1-s)}ds-\frac{1}{We}\theta_0(t) \\ &\approx x_\infty-\frac{1}{\pi}\int_t^{+\infty}\frac{1}{(1-s)}ds. \end{aligned} \tag{34}$$

  and
$$y_0(t)\approx 1-\frac{1}{\pi}\int_t^{+\infty}\frac{\theta_0(s)}{(1-s)}ds-\frac{\theta_0^2(t)}{2We}\approx 1. \tag{35}$$

  On the other hand, we have the formula:
$$x_\infty\approx\frac{1}{\pi}p.v.\int_0^{+\infty}\frac{1}{(1-s)}ds, \tag{36}$$

  hence
$$x_0(t)\approx-\frac{1}{\pi}\ln(t-1). \tag{37}$$

3.2. First-order approximation

Now, we find the first-order approximation of the nonlinear integral equations (25), (28)–(30) by using development (31) and the zero-order approximation of the system.

Using the development (31), we can write

$$X_{1,\alpha_i}(t) \approx \frac{X(t) - X_0(t)}{\alpha_i}. \tag{38}$$

Substituting (25) and (32) into (38) yields

$$q_{1,\alpha_i}(t) \approx \frac{\pi}{We}(t-1)\theta'_{1,\alpha_i}(t). \tag{39}$$

From (28), (33) and (38) we get:

- for $i = -N+1, \ldots, -1$,

$$\theta_{1,\alpha_i}(t) \approx -\frac{\sqrt{t-1}}{We}\int_1^{+\infty} \frac{(s-1)\theta'_{1,\alpha_i}(s)}{(s-t)\sqrt{s-1}}ds + \sum_{i=-N+1}^{-1} \frac{2}{\pi}\tan^{-1}\left(\frac{(m_i - m_{i-1})\sqrt{t-1}}{t-1+m_i m_{i-1}}\right), \tag{40}$$

- for $i = 1, \ldots, N-1$,

$$\theta_{1,\alpha_i}(t) \approx -\frac{\sqrt{t-1}}{We}\int_1^{+\infty} \frac{(s-1)\theta'_{1,\alpha_i}(s)}{(s-t)\sqrt{s-1}}ds - \sum_{i=1}^{N-1} \frac{2}{\pi}\tan^{-1}\left(\frac{(m_{i+1} - m_i)\sqrt{t-1}}{t-1+m_{i+1} m_i}\right). \tag{41}$$

On the other hand, from (29), (30), (35), (37) and (38), we find:

$$x_{1,\alpha_i}(t) \approx -\frac{1}{We}\theta_{1,\alpha_i}(t), \tag{42}$$

and

$$y_{1,\alpha_i}(t) \approx -\frac{1}{\pi}\int_t^{+\infty} \frac{\theta_{1,\alpha_i}(s)}{(1-s)}ds. \tag{43}$$

From (40), (41), and for a very large value of the Weber number We, we may neglect the first term with respect to the second one. Thus, we get the first-order approximation of the velocity direction relative to the horizontal axis:

$$\theta_{1,\alpha_i}(t) \approx \frac{2}{\pi}\arctan\left(\frac{(m_i - m_{i-1})\sqrt{t-1}}{t-1+m_i m_{i-1}}\right), \quad i = -N+1, \ldots, -1, \tag{44}$$

$$\theta_{1,\alpha_i}(t) \approx -\frac{2}{\pi}\arctan\left(\frac{(m_{i+1} - m_i)\sqrt{t-1}}{t-1+m_{i+1} m_i}\right), \quad i = 1, \ldots, N-1. \tag{45}$$

Substituting (44), (45) into (42) and (43) and carrying out the integration, one finds

$$x_{1,\alpha_i}(t) \approx -\frac{2}{\pi We}\arctan\left(\frac{(m_i - m_{i-1})\sqrt{t-1}}{t-1+m_i m_{i-1}}\right), i = -N+1, \ldots, -1, \tag{46}$$

$$x_{1,\alpha_i}(t) \approx \frac{2}{\pi We}\arctan\left(\frac{(m_{i+1} - m_i)\sqrt{t-1}}{t-1+m_{i+1} m_i}\right), \quad i = 1, \ldots, N-1, \tag{47}$$

and

$$y_{1,\alpha_i}(t) \approx \frac{4\,(m_i - m_{i-1})}{\pi^2\sqrt{m_i m_{i-1}}}\arctan\left(\sqrt{\frac{m_i m_{i-1}}{t-1}}\right), \quad i = -N+1, \ldots, -1, \tag{48}$$

$$y_{1,\alpha_i}(t) \approx -\frac{4\,(m_{i+1}-m_i)}{\pi^2\sqrt{m_{i+1}m_i}}\arctan\left(\sqrt{\frac{m_{i+1}m_i}{t-1}}\right), \quad i=1,\ldots,N-1. \tag{49}$$

Using results (35), (37), (46)–(49) and expanding (31) enables finding the approximate solutions of the free-surface flow:

$$\begin{aligned} x(t) \;\approx\; & -\frac{1}{\pi}\ln(t-1) - \sum_{i=-N+1}^{-1}\frac{2\alpha_i}{\pi We}\tan^{-1}\left(\frac{(m_i-m_{i-1})\sqrt{t-1}}{t-1+m_i m_{i-1}}\right) \\ & + \sum_{i=1}^{N-1}\frac{2\alpha_i}{\pi We}\tan^{-1}\left(\frac{(m_{i+1}-m_i)\sqrt{t-1}}{t-1+m_{i+1}m_i}\right), \end{aligned} \tag{50}$$

and

$$\begin{aligned} y(t) \;\approx\; & 1+\sum_{i=-N+1}^{-1}\frac{4\,(m_i-m_{i-1})\,\alpha_i}{\pi^2\sqrt{m_i m_{i-1}}}\tan^{-1}\left(\sqrt{\frac{m_i m_{i-1}}{t-1}}\right) \\ & - \sum_{i=1}^{N-1}\frac{4\,(m_{i+1}-m_i)\,\alpha_i}{\pi^2\sqrt{m_{i+1}m_i}}\tan^{-1}\left(\sqrt{\frac{m_{i+1}m_i}{t-1}}\right), \quad t>1. \end{aligned} \tag{51}$$

4. Application example for $N=2$ and $\alpha_{-2}=\alpha_2=0$

The previous approximate scheme is used to calculate the solutions and the free surface profiles for fixed values of flow with large Weber number are found throughout a range of different Weber number. The Fig. 4 presented the variation of the free surface shape with respect to the Weber number, fixed the angles values $\alpha_{-1}=\alpha_1=\pi/6$, $l_{-2}=l_2=1$, and the depth of the obstacle value $r_{-1}=0.65$.

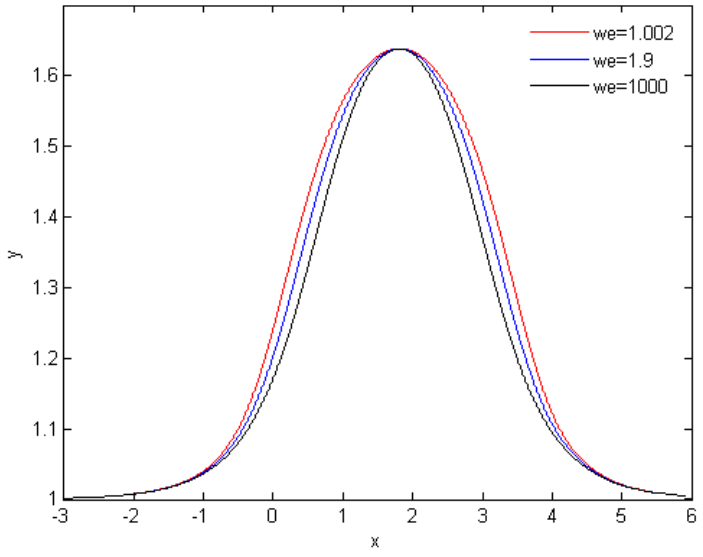

Fig. 4. Effect of Weber number on the free-surface profile at a fixed the trapezoid depth $r_{-1}=0.65$ and the angles $\alpha_{-1}=\pi/6$, $\alpha_1=\pi/6$.

As presented in Fig. 4, the curvature of the free surface is decreased if the Weber number decreases, because this is an important characteristic property of the surface tension effects. The

free-surface profiles for four different depths r_{-1} are plotted in Fig. 5 at a fixed Weber number $We = 200$, $l_{-2} = l_2 = 1$, $\alpha_{-1} = \alpha_1 = \frac{\pi}{8}$. This clarifies that increasing the depth r_{-1} results in more deviation of the free surface from the horizontal one.

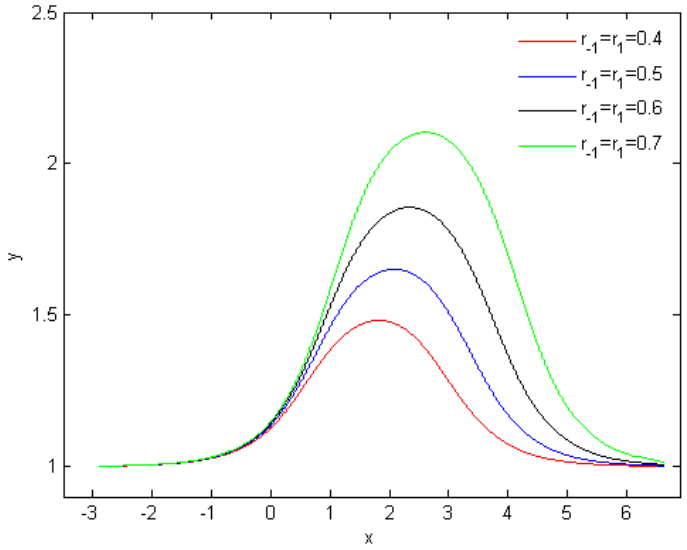

Fig. 5. Effect of the trapezoid depth r_{-1} on the free-surface profile Weber number $We = 200$ and the angles $\alpha_{-1} = \alpha_1 = \pi/8$

Fig. 6 shows the free-surface profiles for different angles α_1 at a fixed $\alpha_{-1} = \pi/8$,$r_{-1} = 0.5$, and at a fixed Weber number $We = 200$. Fig. 6 shows the free-surface profiles for four different angles α_{-1} at a fixed $\alpha_1 = \pi/6$,$r_{-1} = 0.5$ and at a fixed Weber number $We = 200$.

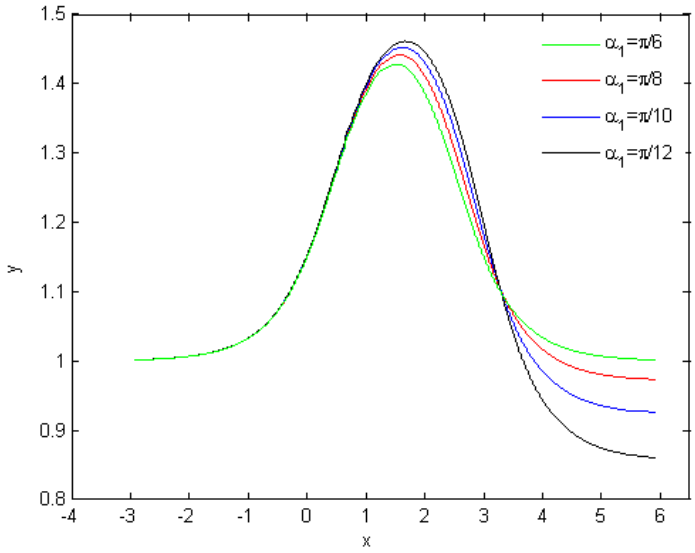

Fig. 6. Effect of the angles α_1 on the free-surface profile Weber number $We = 200$, the angle $\alpha_{-1} = \pi/6$ and the trapezoid depth $r_{-1} = 0.5$

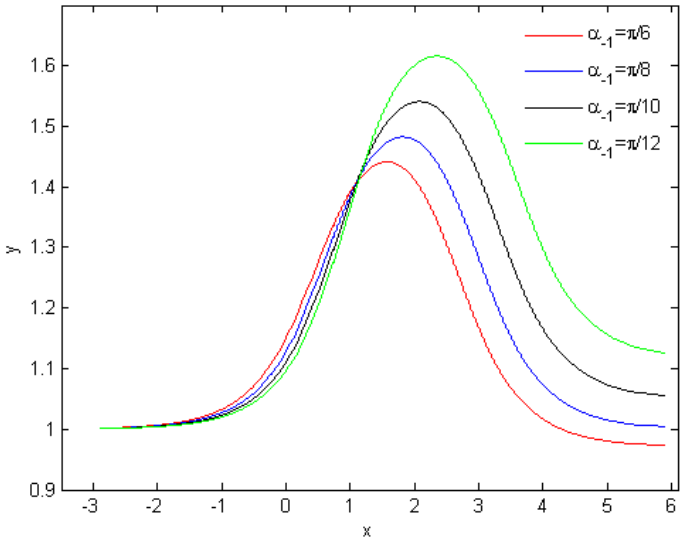

Fig. 7. Effect of the angles α_{-1} on the free-surface profile Weber number $We = 200$, the angle $\alpha_1 = \pi/8$ and the trapezoid depth $r_{-1} = 0.5$

The two Fig. 6 and 7 evidently show that the deviation of the free-surface results from the change in angles.

Conclusion

In this paper, the problem of flow over a trapezoidal obstacle is formulated as a system of nonlinear integral equations. The perturbation technique is used to give an approximate solution to this system for a large Weber number; the free surface profiles under the effect of small surface tension and bottom configurations are illustrated and plotted. The obtained results demonstrate that the used method is easily applicable, and provides approximate solutions to these kinds of problems.

References

[1] L.K.Forbes, L.W.Schwartz, Free-surface flow over a semicircular obstruction, *J. Fluid Mech*, **114**(1982), 299–314.

[2] A.Gasmi, H.Mekias, The effect of surface tension on the contraction coefficient of a jet, *J. Phys. A: Math. Gen*, **36**(2003), 851–862.

[3] A.Gasmi, A.Amara, Free-surface profile of a jet flow in U-shaped channel without gravity effects, *ASCM (Kyungshang)*, **28**(2018), no. 3, 393–400.

[4] J-M.Vanden-Broeck, J.Marc, Free-surface flow over an obstruction in a channel, *The Physics of fluids*, **30**(1987), no. 8, 2315–2317.

[5] F.Dias, J.B.Keller, J.M Vanden-Broeck, Flows over rectangular weirs, *The Physics of fluids*, **31**(1988), no. 8, 2071–2076.

[6] L.Wiryanto, Zero gravity of free-surface flow under a sluice gate, Journal of Physics: Conference Series. IOP Publishing, 2020.

[7] M.B.Abd-el Malek, S.Z.Masoud, Linearized solution of a flow over a ramp, *Appl. Math. Model*, **12**(1988), no. 4, 406–410.

[8] M.B.Abd-el Malek, S.N.Hanna, Approximate solution of a flow over a ramp for large Froude number,*J. Comput. Appl. Math*,**28**(1989), 105–117.

[9] M.B.Abd-el Malek, S.N.Hanna, M.T.Kamel, Approximate solution of gravity flow from a uniform channel over triangular bottom for large Froude number, *Appl. Math. Model*, **15**(1991), no. 1, 25–32.

[10] M.M.Bounif, A.Gasmi, First order perturbation approach for the free surface flow over a step with large Weber number, *INCAS Bulletin*, **13**(2021), no. 2, 11–19.

[11] C.S.Song, A Quasi–Linear and Linear Theory for Non-Separated and Separated Two-Dimensional, Incompressible Irrotational Flow about Lifting Bodies, St. Anthony Falls Hydraulic Laboratory, 1963.

Метод возмущений при обтекании трапециевидного препятствия

Май Манал Боуниф
Абделькадеф Газми
Лаборатория чистой и прикладной математики
Факультет математики и информатики
Университет Мсила
Мсила, Алжир

Аннотация. В этой статье мы рассматриваем двумерное и безвихревое течение невязкой и несжимаемой жидкости над трапециевидным препятствием. Свободная поверхность обтекателя регулируется условием Бернулли, которое определяется в рамках решения задачи. Это условие затрудняет аналитическое решение проблемы. Следовательно, цель нашей работы — использовать преобразование Герберта и технику возмущений, чтобы обеспечить приближенное решение этой проблемы для больших чисел Вебера и различных конфигураций препятствия. Полученные результаты показывают, что используемый метод прост в применении и дает приблизительные решения подобных задач.

Ключевые слова: свободный поверхностный поток, поверхностное натяжение, несжимаемый поток, метод Гильберта, возмущение техника.